

# Chiral family classification of fermionic $Z_2 \times Z_2$ heterotic orbifold models

Alon E. Faraggi<sup>a,\*</sup>, Costas Kounnas<sup>b,1</sup>, John Rizos<sup>c</sup>

<sup>a</sup> *Department of Mathematical Sciences, University of Liverpool, Liverpool L69 7ZL, UK*

<sup>b</sup> *Laboratoire de Physique Théorique, Ecole Normale Supérieure, F-75231 Paris 05, France*

<sup>c</sup> *Department of Physics, University of Ioannina, GR-45110 Ioannina, Greece*

Received 5 July 2006; received in revised form 9 August 2006; accepted 31 August 2006

Available online 22 February 2007

Editor: G.F. Giudice

## Abstract

Free fermionic construction of four-dimensional string vacua, are related to the  $Z_2 \times Z_2$  orbifolds at special points in the moduli space, and yielded the most realistic three family string models to date. Using free fermionic construction techniques we are able to classify more than  $10^{10}$  string vacua by the net family and anti-family number. Using a Monte Carlo technique we find a bell shaped distribution that peaks at vanishing net number of chiral families. We also observe that  $\sim 15\%$  of the models have three net chiral families. In addition to mirror symmetry we find that the distribution exhibits a symmetry under the exchange of (spinor plus anti-spinor) representations with vectorial representations.

© 2007 Elsevier B.V. All rights reserved.

## 1. Introduction

The four-dimensional superstring vacua based on the free fermionic construction [1] are  $Z_2 \times Z_2$  toroidal orbifolds at special points in the moduli space [2,3]. The correspondence of the free fermionic point in the moduli space to T-self-dual points with maximally enhanced symmetries suggests that symmetry enhancement and self-duality play a role in the string vacuum selection. Furthermore, the three generation heterotic string models [4] in the free fermionic formulation [1] are the most realistic string models constructed to date. The phenomenological appeal, and the theoretical considerations, motivate the elaborate study of this class of string compactifications.

We have therefore embarked in Ref. [5] on a complete classification of symmetric  $Z_2 \times Z_2$  free fermionic orbifold models, according to the chiral content and the four-dimensional matter gauge group. Thanks to the observation [5] that the twisted matter in the models does not depend on the moduli, their chi-

rality classification can be carried out at the free fermionic point of the moduli space. Thus, this enables utilizing free fermionic techniques, which allows an algorithm adaptable to a computer program. Resorting to the well-known relations in two dimensions between fermionic and bosonic currents, one can find the translation of the partition function in the bosonic and fermionic representation, and this for any arbitrary point of the moduli space. Hence, the free fermionic analysis enables the chirality classification of all symmetric, as well as the asymmetric,  $Z_2 \times Z_2$  orbifolds. Thus, the free fermionic formalism provides powerful tools for the complete classification of  $Z_2 \times Z_2$  perturbative string orbifolds.

The general techniques for carrying out such a classification in the free fermionic language were developed in Ref. [6] for type II string, and applied in Ref. [5] for the classification of heterotic chiral  $Z_2 \times Z_2$  models. The analysis in Ref. [5] was performed with respect to a subclass of the models. The  $Z_2 \times Z_2$  orbifold of a six-dimensional compact manifold contains three twisted sectors. In the heterotic string each one of these sectors may, or may not, a priori (prior to application of the Generalized GSO (GGSO) projections), give rise to spinorial representations. Models that may produce, a priori, spinorial representations from all three twisted sectors were dubbed  $S^3$  models. This class was classified in Ref. [5].

\* Corresponding author.

E-mail address: [faraggi@sune.amtp.liv.ac.uk](mailto:faraggi@sune.amtp.liv.ac.uk) (A.E. Faraggi).

<sup>1</sup> Unité Mixte de Recherche (UMR 8549) du CNRS et de l'ENS associée à l'université Pierre et Marie Curie.

It is also possible that the spinorial representations are not present in a given twisted plane. Thus, generically we may classify the models in four distinct classes:  $S^3$ ,  $S^2V$ ,  $SV^2$  and  $V^3$  classes of models with spinorial representations arising from three, two, one or none of the twisted sectors, respectively. The aim of this work is to go beyond the analysis of Ref. [5] and complete the chirality classification of the  $Z_2 \times Z_2$  symmetric orbifolds.

In this process we find several surprising results. One can envision performing the classification by removing or modifying some vectors from the basis set which was utilized in Ref. [5], in such a way that only two, one or none of the twisted sectors produces massless spinorial representations. This method was pursued in Ref. [7]. However, it is found that the entire sets of  $S^3$ ,  $S^2V$ ,  $SV^2$  and  $V^3$  classes of models are produced by working with the basis set of Ref. [5] for certain choices of the one-loop GGSO projection coefficients (discrete torsions). This result arises from theta function identities in the one-loop partition function, which we exhibit in the simplest case as an illustration. Hence, these identities allow a complete classification of the free fermionic  $Z_2 \times Z_2$  orbifold models using a single set of boundary condition basis vectors and varying the phases. This enables a systematic analysis of the models and the production of algebraic formulas for the main features of the models like the number of spinorial, anti-spinorial and vectorial representations. While in the past the studies of phenomenologically relevant free fermionic string models has been confined to isolated examples, the new methodology allows us to scan a range of over  $10^{16}$  models, and therefore obtain vital insight into the properties of the entire space of  $Z_2 \times Z_2$  orbifold vacua. In this Letter we present the main outline of the analysis and highlights of the results. Further details and results will be reported in a forthcoming publication.

## 2. Review of the classification method

In the free fermionic formulation the 4-dimensional heterotic string, in the light-cone gauge, is described by 20 left-moving and 44 right-moving two-dimensional real fermions [1]. A large number of models can be constructed by choosing different phases picked up by fermions ( $f_A$ ,  $A = 1, \dots, 44$ ) when transported along the torus non-contractible loops. Each model corresponds to a particular choice of fermion phases consistent with modular invariance that can be generated by a set of basis vectors  $v_i$ ,  $i = 1, \dots, n$ ,

$$v_i = \{\alpha_i(f_1), \alpha_i(f_2), \alpha_i(f_3), \dots\}$$

describing the transformation properties of each fermion

$$f_A \rightarrow -e^{i\pi\alpha_i(f_A)} f_A, \quad A = 1, \dots, 44. \quad (2.1)$$

The basis vectors span a space  $\mathcal{E}$  which consists of  $2^N$  sectors that give rise to the string spectrum. Each sector is given by

$$\xi = \sum N_i v_i, \quad N_i = 0, 1. \quad (2.2)$$

The spectrum is truncated by a GGSO projection whose action on a string state  $|S\rangle$  is

$$e^{i\pi v_i \cdot F_S} |S\rangle = \delta_S c \begin{bmatrix} S \\ v_i \end{bmatrix} |S\rangle, \quad (2.3)$$

where  $F_S$  is the fermion number operator and  $\delta_S = \pm 1$  is the space–time spin statistics index. Different sets of projection coefficients  $c \begin{bmatrix} S \\ v_i \end{bmatrix} = \pm 1$  consistent with modular invariance give rise to different models. Summarizing: a model can be defined uniquely by a set of basis vectors  $v_i$ ,  $i = 1, \dots, n$ , and a set of  $2^{N(N-1)/2}$  independent projections coefficients  $c \begin{bmatrix} v_i \\ v_j \end{bmatrix}$ ,  $i > j$ .

The two-dimensional free fermions in the light-cone gauge (in the usual notation) are:  $\psi^\mu, \chi^i, y^i, \omega^i$ ,  $i = 1, \dots, 6$  (real left-moving fermions) and  $\bar{y}^i, \bar{\omega}^i$ ,  $i = 1, \dots, 6$  (real right-moving fermions),  $\psi^A$ ,  $A = 1, \dots, 5$ ,  $\bar{\eta}^B$ ,  $B = 1, 2, 3$ ,  $\bar{\phi}^\alpha$ ,  $\alpha = 1, \dots, 8$  (complex right-moving fermions). The class of models under investigation is generated by a set  $V$  of 12 basis vectors

$$V = \{v_1, v_2, \dots, v_{12}\},$$

where

$$\begin{aligned} v_1 = 1 &= \{\psi^\mu, \chi^{1,\dots,6}, y^{1,\dots,6}, \omega^{1,\dots,6} | \\ &\quad \bar{y}^{1,\dots,6}, \bar{\omega}^{1,\dots,6}, \bar{\eta}^{1,2,3}, \bar{\psi}^{1,\dots,5}, \bar{\phi}^{1,\dots,8}\}, \\ v_2 = S &= \{\psi^\mu, \chi^{1,\dots,6}\}, \\ v_{2+i} = e_i &= \{y^i, \omega^i | \bar{y}^i, \bar{\omega}^i\}, \quad i = 1, \dots, 6, \\ v_9 = b_1 &= \{\chi^{34}, \chi^{56}, y^{34}, y^{56} | \bar{y}^{34}, \bar{y}^{56}, \bar{\eta}^1, \bar{\psi}^{1,\dots,5}\}, \\ v_{10} = b_2 &= \{\chi^{12}, \chi^{56}, y^{12}, y^{56} | \bar{y}^{12}, \bar{y}^{56}, \bar{\eta}^2, \bar{\psi}^{1,\dots,5}\}, \\ v_{11} = z_1 &= \{\bar{\phi}^{1,\dots,4}\}, \\ v_{12} = z_2 &= \{\bar{\phi}^{5,\dots,8}\}. \end{aligned} \quad (2.4)$$

The vectors  $1, S$  generate an  $N = 4$  supersymmetric model. The vectors  $e_i$ ,  $i = 1, \dots, 6$ , give rise to all possible symmetric shifts of the six internal fermionized coordinates ( $\partial X^i = y^i \omega^i$ ,  $\bar{\partial} X^i = \bar{y}^i \bar{\omega}^i$ ), while  $b_1$  and  $b_2$  define the  $Z_2 \times Z_2$  orbifold twists. The remaining fermions not affected by the action of the previous vectors  $\{S, e^i, b_i\}$  are  $\bar{\phi}^i$ ,  $i = 1, \dots, 8$ , which normally give rise to the hidden sector gauge group. The vectors  $z_1, z_2$  divide these eight complex fermions into two sets of four. We stress here that the choice of  $V$  is the most general set of basis vectors, with symmetric shifts for the internal fermions, compatible with a Kac–Moody level one  $SO(10)$  embedding. Without loss of generality we can fix the associated projection coefficients

$$\begin{aligned} c \begin{bmatrix} 1 \\ 1 \end{bmatrix} &= c \begin{bmatrix} 1 \\ S \end{bmatrix} = c \begin{bmatrix} S \\ S \end{bmatrix} = c \begin{bmatrix} S \\ e_i \end{bmatrix} = c \begin{bmatrix} S \\ b_A \end{bmatrix} \\ &= -c \begin{bmatrix} b_2 \\ S \end{bmatrix} = c \begin{bmatrix} S \\ z_n \end{bmatrix} = -1, \end{aligned}$$

leaving 55 independent coefficients,

$$\begin{aligned} c \begin{bmatrix} e_i \\ e_j \end{bmatrix}, \quad i \geq j, \quad c \begin{bmatrix} b_1 \\ b_2 \end{bmatrix}, \quad c \begin{bmatrix} z_1 \\ z_2 \end{bmatrix}, \\ c \begin{bmatrix} e_i \\ z_n \end{bmatrix}, \quad c \begin{bmatrix} e_i \\ b_A \end{bmatrix}, \quad c \begin{bmatrix} b_A \\ z_n \end{bmatrix}, \quad i, j = 1, \dots, 6, \end{aligned}$$

$A, B, m, n = 1, 2,$

since the remaining projection coefficients are determined by modular invariance [1]. Each of the 55 independent coefficients can take two discrete values  $\pm 1$  and thus a simple counting gives  $2^{55}$  (that is approximately  $10^{16.6}$ ) distinct models in the class of superstring vacua under consideration.

The vector bosons from the untwisted sector generate an  $SO(10) \times U(1)^3 \times SO(8)^2$  gauge symmetry. Depending on the choices of the projection coefficients, extra gauge bosons may arise from

$$x = 1 + S + \sum_{i=1}^6 e_i + z_1 + z_2 = \{\bar{\eta}^{123}, \bar{\psi}^{12345}\}$$

changing the gauge group  $SO(10) \times U(1) \rightarrow E_6$ . Additional gauge bosons can arise as well from the sectors  $z_1, z_2$  and  $z_1 + z_2$  and enhance the hidden gauge group  $SO(8)^2 \rightarrow SO(16)$  or even  $SO(8)^2 \rightarrow E_8$ . Indeed, as was shown in Ref. [5], for particular choices of the projection coefficients a variety of gauge groups is obtained.

The matter spectrum from the untwisted sector is common to all models and consists of six vectors of  $SO(10)$  and 12 non-Abelian gauge group singlets. The chiral spinorial representations arise from the following 48 twisted sectors

$$\begin{aligned} B_{\ell_3^1 \ell_4^1 \ell_5^1 \ell_6^1}^1 &= S + b_1 + \ell_3^1 e_3 + \ell_4^1 e_4 + \ell_5^1 e_5 + \ell_6^1 e_6, \\ B_{\ell_1^2 \ell_2^2 \ell_3^2 \ell_6^2}^2 &= S + b_2 + \ell_1^2 e_1 + \ell_2^2 e_2 + \ell_3^2 e_5 + \ell_6^2 e_6, \\ B_{\ell_1^3 \ell_2^3 \ell_3^3 \ell_4^3}^3 &= S + b_3 + \ell_1^3 e_1 + \ell_2^3 e_2 + \ell_3^3 e_3 + \ell_4^3 e_4, \end{aligned} \quad (2.5)$$

where  $\ell_i^j = 0, 1$  and  $b_3 = 1 + S + b_1 + b_2 + \sum_{i=1}^6 e_i + \sum_{n=1}^2 z_n$ . These states are spinorials of  $SO(10)$  and one can obtain at maximum one spinorial (**16** or  $\overline{\mathbf{16}}$ ) per sector and thus totally 48 spinorials. Extra non-chiral matter, i.e. vectors of  $SO(10)$  as well as singlets, arise from the  $B_{\ell_3^i \ell_4^i \ell_5^i \ell_6^i}^i + x$  ( $i = 1, 2, 3$ ) twisted sectors.

This construction therefore separates the fixed points of the  $Z_2 \times Z_2$  orbifold into different sectors. This enables the analysis of the GGSO projection on the spectrum from each individual fixed point separately. Hence, depending on the choice of the GGSO projection coefficients we can distinguish several possibilities for the spectrum from each individual fixed point. For example, in the case of enhancement of the  $SO(10)$  symmetry to  $E_6$  each individual fixed point gives rise to spinorial as well as vectorial representation of  $SO(10)$  which are embedded in the 27 representation of  $E_6$ . When  $E_6$  is broken each fixed point typically will give rise to either spinorial or vectorial representation of  $E_6$ . However, there exist also rare situations, depending on the choice of GGSO phases, where a fixed point can yield a spinorial as well as vectorial representation of  $SO(10)$  without enhancement. The crucial point, however, is that the GGSO projections can be written as simple algebraic conditions, and hence the classification is amenable to a computerized analysis.

In Ref. [5] we restricted the analysis to the case  $c\left[\begin{smallmatrix} z_1 \\ z_2 \end{smallmatrix}\right] = -1$ . Prior to GGSO projections spinorial representations in this construction can arise from all three twisted sectors and we therefore referred to this class as  $S^3$  models. This is somewhat of a

misnomer as we discuss below. To produce models with spinorial representations arising only from one or two of the twisted one can contemplate modifying the basis vectors. For example, removing  $z_2$  from the set will entail that the third twisted place produces only massive states. Hence, this would correspond to the models dubbed as  $S^2V$ . Similarly, modifying the  $Z_2 \times Z_2$  basis vectors  $b_1$  and  $b_2$  in such a way that they produce vectorial rather than spinorial representation and removing both  $z_1$  and  $z_2$  from the base would entail that only vectorial representations are generated. An analysis along this lines was followed in Ref. [7]. However, as a result of Jacobi theta function identities it turns out that the analysis can be carried entirely with the basis (2.4) and just modifying the phases. To illustrate this correspondence we consider the simplest possibility given by the set  $\{1, S, x\}$ . The partition function is

$$\{\theta_3^4 - \theta_2^4 - \theta_4^4\} \{\theta_3^6 \bar{\theta}_3^{14} + \theta_2^6 \bar{\theta}_2^{14} + \theta_4^6 \bar{\theta}_4^{14}\} \{\bar{\theta}_2^8 + \bar{\theta}_3^8 + \bar{\theta}_4^8\}. \quad (2.6)$$

The gauge group is  $SO(28) \times E_8$ . Now consider the set  $\{1, S, x, z_1\}$ . There are now two consistent choices of the coefficient  $c\left[\begin{smallmatrix} x \\ z_1 \end{smallmatrix}\right] = \pm 1$ . The choice  $c\left[\begin{smallmatrix} x \\ z_1 \end{smallmatrix}\right] = +1$  produces the  $SO(28) \times E_8$  gauge group, while the choice  $c\left[\begin{smallmatrix} x \\ z_1 \end{smallmatrix}\right] = -1$  produces an  $SO(20) \times SO(24)$  gauge group. Indeed, the one-loop partition function as function of  $c\left[\begin{smallmatrix} x \\ z_1 \end{smallmatrix}\right]$  becomes

$$\begin{aligned} &\frac{1}{2} \{\theta_3^4 - \theta_2^4 - \theta_4^4\} \{\theta_3^6 \bar{\theta}_3^{10}\} \left\{ \bar{\theta}_3^4 \bar{\theta}_2^8 + \bar{\theta}_3^4 \bar{\theta}_3^8 + \bar{\theta}_3^4 \bar{\theta}_4^8 \right. \\ &\quad \left. + c\left[\begin{smallmatrix} z_1 \\ x \end{smallmatrix}\right] \bar{\theta}_4^4 \bar{\theta}_2^8 + \bar{\theta}_4^4 \bar{\theta}_3^8 + \bar{\theta}_4^4 \bar{\theta}_4^8 \right. \\ &\quad \left. + \bar{\theta}_2^4 \bar{\theta}_2^8 + \bar{\theta}_2^4 \bar{\theta}_3^8 + c\left[\begin{smallmatrix} z_1 \\ x \end{smallmatrix}\right] \bar{\theta}_2^4 \bar{\theta}_4^8 \right\} + \dots \end{aligned}$$

plus two additional groups of terms with the permutation of  $\bar{\theta}_3, \bar{\theta}_2$  and  $\bar{\theta}_4$ . Fixing  $c\left[\begin{smallmatrix} z_1 \\ x \end{smallmatrix}\right] = +1$  and using the Jacobi identity  $\bar{\theta}_3^4 - \bar{\theta}_2^4 - \bar{\theta}_4^4 \equiv 0$  reproduces the partition function of the set  $\{1, S, x\}$ . This simple example illustrates how we may obtain vacua from an enlarged basis set  $\{1, S, x, z_1\}$  identical to those obtained from a reduced basis set  $\{1, S, x\}$  for an appropriate choice of the GGSO coefficient  $c\left[\begin{smallmatrix} z_1 \\ x \end{smallmatrix}\right]$ , and is the primary feature which is exploited in our classification.

### 3. Counting the twisted matter spectrum

The counting of spinorials can proceed as follows. For each  $SO(10)$  spinorial  $B_{pqrs}^i$  in (2.5) we write down the associated projector  $P_{pqrs}^i = 0, 1$ . The detailed expressions for the 48 projectors are

$$\begin{aligned} P_{\ell_3 \ell_4 \ell_5 \ell_6}^{(1)} &= \frac{1}{4} \left( 1 - c\left[\begin{smallmatrix} e_1 \\ B_{\ell_3 \ell_4 \ell_5 \ell_6}^{(1)} \end{smallmatrix}\right] \right) \left( 1 - c\left[\begin{smallmatrix} e_2 \\ B_{\ell_3 \ell_4 \ell_5 \ell_6}^{(1)} \end{smallmatrix}\right] \right) \\ &\quad \times \frac{1}{4} \left( 1 - c\left[\begin{smallmatrix} z_1 \\ B_{\ell_3 \ell_4 \ell_5 \ell_6}^{(1)} \end{smallmatrix}\right] \right) \left( 1 - c\left[\begin{smallmatrix} z_2 \\ B_{\ell_3 \ell_4 \ell_5 \ell_6}^{(1)} \end{smallmatrix}\right] \right), \\ P_{\ell_1 \ell_2 \ell_5 \ell_6}^{(2)} &= \frac{1}{4} \left( 1 - c\left[\begin{smallmatrix} e_3 \\ B_{\ell_1 \ell_2 \ell_5 \ell_6}^{(2)} \end{smallmatrix}\right] \right) \left( 1 - c\left[\begin{smallmatrix} e_4 \\ B_{\ell_1 \ell_2 \ell_5 \ell_6}^{(2)} \end{smallmatrix}\right] \right) \\ &\quad \times \frac{1}{4} \left( 1 - c\left[\begin{smallmatrix} z_1 \\ B_{\ell_1 \ell_2 \ell_5 \ell_6}^{(2)} \end{smallmatrix}\right] \right) \left( 1 - c\left[\begin{smallmatrix} z_2 \\ B_{\ell_1 \ell_2 \ell_5 \ell_6}^{(2)} \end{smallmatrix}\right] \right), \end{aligned}$$

$$P_{\ell_1 \ell_2 \ell_3 \ell_4}^{(3)} = \frac{1}{4} \left( 1 - c \left[ B_{\ell_1 \ell_2 \ell_3 \ell_4}^{(3)} \begin{matrix} e_5 \\ \end{matrix} \right] \right) \left( 1 - c \left[ B_{\ell_1 \ell_2 \ell_3 \ell_4}^{(3)} \begin{matrix} e_6 \\ \end{matrix} \right] \right) \\ \times \frac{1}{4} \left( 1 - c \left[ B_{\ell_1 \ell_2 \ell_3 \ell_4}^{(3)} \begin{matrix} z_1 \\ \end{matrix} \right] \right) \left( 1 - c \left[ B_{\ell_1 \ell_2 \ell_3 \ell_4}^{(3)} \begin{matrix} z_2 \\ \end{matrix} \right] \right). \quad (3.1)$$

For the surviving spinorial ( $P_{pqrs}^i = 1$ ) the chirality (**16** or  $\overline{\mathbf{16}}$ ) is determined from the associated chirality coefficient  $X_{pqrs}^i = \pm 1$ , where

$$X_{\ell_1 \ell_2 \ell_5 \ell_6}^{(1)} = -c \left[ \begin{matrix} b_2 + (1 - \ell_5)e_5 + (1 - \ell_6)e_6 \\ B_{\ell_3 \ell_4 \ell_5 \ell_6}^{(1)} \end{matrix} \right], \\ X_{\ell_1 \ell_2 \ell_5 \ell_6}^{(2)} = -c \left[ \begin{matrix} b_1 + (1 - \ell_5)e_5 + (1 - \ell_6)e_6 \\ B_{\ell_1 \ell_2 \ell_5 \ell_6}^{(2)} \end{matrix} \right], \\ X_{\ell_1 \ell_2 \ell_3 \ell_4}^{(3)} = -c \left[ \begin{matrix} b_1 + (1 - \ell_3)e_3 + (1 - \ell_4)e_4 \\ B_{\ell_1 \ell_2 \ell_3 \ell_4}^{(3)} \end{matrix} \right]. \quad (3.2)$$

Using the above results, we can easily calculate the number of spinorials/anti-spinorials per sector

$$S_{\pm}^{(i)} = \sum_{pqrs} \frac{1 \pm X_{pqrs}^{(i)}}{2} P_{pqrs}^{(i)}, \quad i = 1, 2, 3. \quad (3.3)$$

The counting of  $SO(10)$  vectorials can proceed in a similar way. For each vectorial generating sector  $B_{pqrs}^i + x$  the associated projector  $\tilde{P}_{pqrs}^i$  is obtained from (3.1) using the replacement  $B_{pqrs}^i \rightarrow B_{pqrs}^i + x$ . Since there is no chirality in this case the number of vectorials per sector is just the sum of the projectors

$$V^{(i)} = \sum_{pqrs} \tilde{P}_{pqrs}^{(i)}. \quad (3.4)$$

The total vectorial ( $V$ ) and net spinorial ( $S$ ) numbers are

$$V = \sum_{i=1}^3 V^{(i)} \quad (3.5)$$

and

$$S = \sum_{i=1}^3 S_+^{(i)} - S_-^{(i)}. \quad (3.6)$$

The mixed projection coefficients entering the above formulas can be decomposed in terms of the independent phases  $c \left[ \begin{matrix} v_i \\ v_j \end{matrix} \right]$ ,  $i > j$ . After some algebra we come to the conclusion that for the counting of the spinorial/anti-spinorial and vectorial  $SO(10)$  states the phases  $c \left[ \begin{matrix} e_i \\ e_j \end{matrix} \right]$ ,  $i = 1, \dots, 6$ ,  $c \left[ \begin{matrix} z_A \\ z_A \end{matrix} \right]$ ,  $A = 1, \dots, 2$ ,  $c \left[ \begin{matrix} b_I \\ b_I \end{matrix} \right]$ ,  $I = 1, \dots, 2$ , as well as  $c \left[ \begin{matrix} e_3 \\ b_1 \end{matrix} \right]$ ,  $c \left[ \begin{matrix} e_4 \\ b_1 \end{matrix} \right]$ ,  $c \left[ \begin{matrix} e_1 \\ b_2 \end{matrix} \right]$ ,  $c \left[ \begin{matrix} e_2 \\ b_2 \end{matrix} \right]$  are not relevant. Moreover the phase  $c \left[ \begin{matrix} b_1 \\ b_2 \end{matrix} \right]$  is related to the total chirality flip. This leaves a set of 40 independent phases which is still too large for a manageable computer analysis. We therefore resort to a Monte Carlo analysis that generates random choices of phases. The complete classification is currently underway and will be reported in a future publication. In this sense our results are based on a statistical polling, with a sample that correspond to some  $10^{10}$  vacua. We have checked however that increasing the size of the sample by 10% does not alter our results. Therefore our results, while in some sense empirical, are expected to hold for the entire space of vacua.

#### 4. The observable and hidden gauge groups

An important step in the analysis is the determination of the four-dimensional gauge group. In particular, it is important to determine the component of the gauge group which is identified with the observable gauge group. Observable matter then consist of the states that are charged with respect to this gauge group. In our construction the sectors that produce space–time vector bosons include:  $G = \{0, z_1, z_2, z_1 + z_2, x\}$ . The 0 sector gauge bosons produce the gauge group  $SO(10) \times U(1)^3 \times SO(8)^2$ . Depending on the choice of the GGSO projection coefficients the four-dimensional gauge group is enhanced. Since the sectors that produce space–time vector bosons do not break any supersymmetries the classification of the four-dimensional gauge group can be done at the level of the  $N = 4$  vacuum. The addition of the supersymmetry breaking sectors  $b_1$  and  $b_2$  then breaks the  $N = 4$  gauge group to the unbroken gauge group at the  $N = 1$  level. Some of the possibilities at the  $N = 1$  level are listed in Table 1.

Several features are noted from the list. The first five groups are descendants of  $SO(32)$ , whereas the later five are descendants of  $E_8 \times E_8$ . This gross division is controlled by the phase  $c \left[ \begin{matrix} z_1 \\ z_2 \end{matrix} \right]$ . An important point to note, relevant for our classification, is the occurrence of models with several  $SO(10)$  group factors. This arises because of the enhancement of the 0-sector  $SO(8) \times U(1)$  group factors to  $SO(10)$ . In our analysis we define the observable gauge group to be  $SO(10)$  and the chiral matter should be charged under that group. The question arises as to which  $SO(10)$  should be identified as the observable gauge group and the subsequent classification of the chiral and vectorial matter states with respect to that group. In our analysis here we identify the observable  $SO(10)$  symmetry as the one which is generated by the world-sheet fermions  $\tilde{\psi}^{12345}$ . Investigations of other possibilities are left for future work, although our experience with the construction of quasi-realistic string models suggests that the spectrum with respect to other  $SO(10)$  group factors is vectorial rather than spinorial.

We further comment that in our classification the observable GUT gauge group is always  $SO(10)$ . The conditions for enhancement of the gauge group are given in Ref. [5, Eqs. (4.3)–(4.11)]. These conditions are incorporated into our classification routine and cases in which the  $SO(10)$  symmetry is enhanced are rejected.

Table 1  
Typical enhanced gauge groups for a generic model generated by the basis (2.4)

Gauge group
$SO(10) \times SO(18) \times U(1)^2$
$SO(10) \times SO(9)^2 \times U(1)^3$
$SO(10)^2 \times SO(9) \times U(1)^2$
$SO(10)^3 \times U(1)$
$SO(26) \times U(1)^3$
$E_6 \times U(1)^2 \times E_8$
$E_6 \times U(1)^2 \times SO(16)$
$E_6 \times U(1)^2 \times SO(8) \times SO(8)$
$SO(10) \times U(1)^3 \times E_8$
$SO(10) \times U(1)^3 \times SO(16)$

We also note that our classification is with respect to the chiral content of the models, which in the free fermionic models arises from the twisted sectors. The breaking of the GUT  $SO(10)$  symmetry to a subgroup, which can be further broken to the Standard Model gauge group, is achieved in free fermionic models with an additional boundary condition basis. Free fermionic models with quasi-realistic gauge group and chiral family content were produced in the past [4]. The interest in this Letter is in the global properties of a large class of compactifications to which the quasi-realistic free fermionic models belong, but not in producing quasi-realistic spectrum. The classification of free fermionic models with broken  $SO(10)$  GUT symmetry will be pursued in future work.

## 5. Results

The results of the random search are exhibited in Figs. 1 and 2. The first figure shows the percentage of models with a net number of chiral families. The second figure exhibits the total number of vacua on a logarithmic scale over the net number of chiral families. In our sample the peak of the distribution is for a vanishing net number of chiral families. About 15% of the models contain a net number of three chiral or anti-chiral families. By increasing the sample size by 10% we note that these results are not modified.

In Fig. 2 we present scatter plot of the logarithm of the number of models versus the net number of chiral families. The vertical spread arises from variations in the number of vectorial representations in the models. The peak is for vanishing net number of chiral families, and we note that the distribution is symmetric about that point. The plot has a bell shape which recedes for increasing number of chiral families. For net family number above 24 the number of occurrences is small and is not shown on the plot. This reflects that increasing number of chiral families requires that the configurations of the GGSO phases attain higher symmetry and consequently the number of possibilities decreases. Curiously, we note that models with some net number of chiral families do not appear on the plot. For example models with 7, 9, 11, 13, 14, 15, 17, 18, 19 net number of chiral families do not appear in our sample. Thus, these are either very rare or forbidden altogether in symmetric  $Z_2 \times Z_2$  orbifolds. Additional plots and analysis of the data will be presented in a forthcoming publication.

The symmetry about the vanishing number of chiral families is in accordance with mirror symmetry. We note, however, an additional symmetry in the distribution under exchange of *vectorial*, and *spinorial plus anti-spinorial*, representations. The symmetry states that for a model with a given total number of spinorial plus anti-spinorial representations there exist a corresponding model in which the spinorial plus anti-spinorial representations are exchanged with vectorial representations. Ultimately, in the free fermionic language this symmetry reflects a symmetry under a discrete exchange of some GGSO projection coefficients. However, it may have interesting implications in terms of the underlying geometrical data.

In conclusion, the quasi-realistic free fermionic models are among the most realistic string models constructed to date.

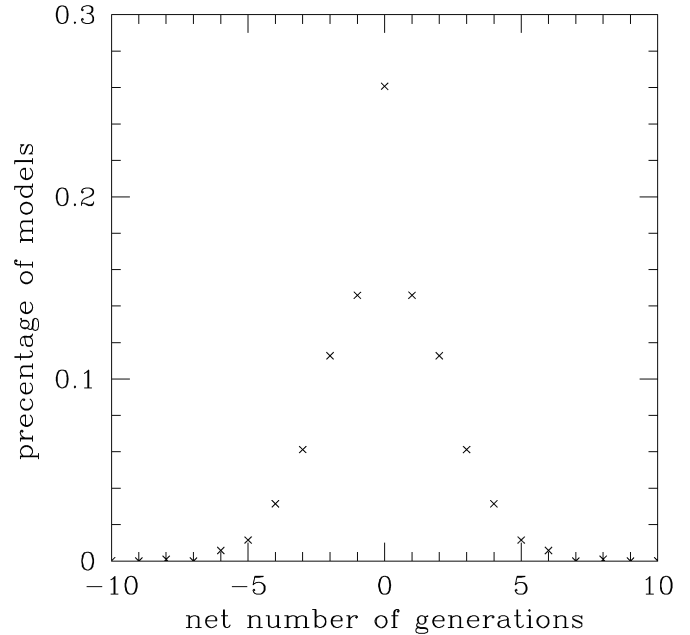


Fig. 1. Distribution of a Monte Carlo generation of models sampling some  $10^{10}$  vacua.

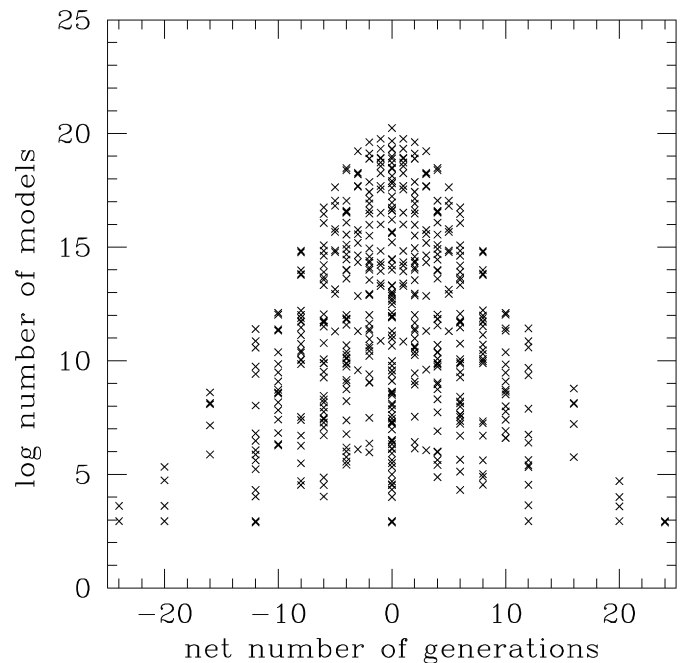


Fig. 2. Scatter plot of the logarithm of the number of models versus the net number of chiral families.

While past exploration of these models consisted of the study of single examples, in this Letter we embarked on the investigation of the properties of the whole space of vacua in this class. Future studies will incorporate into the analysis further properties of the realistic models, like the assignment of asymmetric boundary conditions. While the task is still horrendous in terms of the sheer number of vacua, the existence of string models in this class that come close to describing reality, and precisely

where one would most expect to find them, gives ample reason to suggest that we are on the right track.

### Acknowledgements

We would like to thank Sander Nooij for collaboration at the initial stages of this work. A.E.F. would like to thank the Ecole Normale Supérieure and the University of Ioannina, C.K. would like to thank the University of Ioannina and J.R. would like to thank the Ecole Normale Supérieure, for hospitality. A.E.F. is supported in part by PPARC under contract PP/D000416/1. C.K. is supported in part by the EU under contracts MTRN-CT-2004-005104, MTRN-CT-2004-512194 and ANR (CNRS-USAR) contract No. 05-BLAN-0079-01 (01/12/05). J.R. is supported by the program “PYTHAGORAS” (No. 1705 project 23) of the Operational Program for Education and Initial Vocational Training of the Hellenic Ministry of Education under the 3rd Community Support Framework and the European Social Fund and by the EU under contract MRTN-CT-2004-503369.

### References

- [1] I. Antoniadis, C. Bachas, C. Kounnas, P. Windey, Phys. Lett. B 171 (1986) 51;  
H. Kawai, D.C. Lewellen, S.H.-H. Tye, Nucl. Phys. B 288 (1987) 1;
- I. Antoniadis, C. Bachas, C. Kounnas, Nucl. Phys. B 289 (1987) 87;
- I. Antoniadis, C. Bachas, Nucl. Phys. B 298 (1988) 586.
- [2] A.E. Faraggi, Phys. Lett. B 326 (1994) 62;  
P. Berglund, et al., Phys. Lett. B 433 (1998) 269;  
P. Berglund, et al., Int. J. Mod. Phys. A 15 (2000) 1345;  
R. Donagi, A.E. Faraggi, Nucl. Phys. B 694 (2004) 187.
- [3] E. Kiritsis, C. Kounnas, P.M. Petropoulos, J. Rizos, hep-th/9605011;  
E. Kiritsis, C. Kounnas, P.M. Petropoulos, J. Rizos, Nucl. Phys. B 483 (1997) 141;  
E. Kiritsis, C. Kounnas, Nucl. Phys. B 503 (1997) 117;  
A. Gregori, C. Kounnas, J. Rizos, Nucl. Phys. B 549 (1999) 16;  
A. Gregori, C. Kounnas, Nucl. Phys. B 560 (1999) 135.
- [4] I. Antoniadis, J. Ellis, J. Hagelin, D.V. Nanopoulos, Phys. Lett. B 231 (1989) 65;  
A.E. Faraggi, D.V. Nanopoulos, K. Yuan, Nucl. Phys. B 335 (1990) 347;  
I. Antoniadis, G.K. Leontaris, J. Rizos, Phys. Lett. B 245 (1990) 161;  
A.E. Faraggi, Phys. Lett. B 278 (1992) 131;  
A.E. Faraggi, Nucl. Phys. B 387 (1992) 239;  
G.B. Cleaver, A.E. Faraggi, D.V. Nanopoulos, Phys. Lett. B 455 (1999) 135;  
G.K. Leontaris, J. Rizos, Nucl. Phys. B 554 (1999) 3.
- [5] A.E. Faraggi, C. Kounnas, S.E.M. Nooij, J. Rizos, hep-th/0311058;  
A.E. Faraggi, C. Kounnas, S.E.M. Nooij, J. Rizos, Nucl. Phys. B 695 (2004) 41.
- [6] A. Gregori, C. Kounnas, J. Rizos, Nucl. Phys. B 549 (1999) 16.
- [7] S.E.M. Nooij, hep-th/0603035.